Progress In Electromagnetics Research M, Vol. 83, 9–18, 2019

Reduction of Mobile Phone Radiation Exposure Using Multi-Stopband Frequency Selective Surface

Gouri S. Paul[1], Kaushik Mandal[2, *], Juin Acharjee[3], and Partha P. Sarkar[4]

Abstract—Here, a multi-stopband frequency selective surface (FSS), covering commercial frequency bands CDMA, GSM-900, GSM-1800, LTE-2200 MHz, Wi-Fi, and Bluetooth for mobile communication applications has been proposed employing a pair of concentric square ring patches as a unit cell. Possibilities of annular ring patch type FSS are explored first. Finally, the design comes up with a compact square ring patch type single layer FSS. It is also explored that by increasing the width of the inner ring, operating bandwidth can be enhanced to cover closely spaced commercial frequency bands in a single band. Thereby the mutual coupling between the closely spaced resonators for multiple bands can be minimized. The proposed design is flexible enough to tune the desired resonance frequency by changing the length of the individual ring resonators. The design concept has been formulated using linear polynomial regression (LPR) techniques and validated through proper measurement of the fabricated prototype. This FSS can be used as a mobile back cover to protect mobile users from harmful radiations.

1. INTRODUCTION

Frequency selective surfaces (FSSs) are basically two-dimensional arrays of patches on a dielectric slab or that of apertures within a metallic screen to perform the desired filtering operation [1]. There are some other FSSs made of only dielectrics [2–4] which are useful for large bandwidth, wideband near-field correction, and beam-scanning applications, respectively. Though the use of traditional LC filters fulfills the requirement of a filtering system in some cases, its use is not suitable at all situations. Its failure in multi-functional performance is one of the main drawbacks. FSSs have been studied more than 50 years. They are widely used as antenna reflectors [5], radomes [6], electromagnetic absorbers [7], radar cross section (RCS) reducing element [8], and artificial magnetic conductors [9] due to their band-pass or band-stop responses. Use of FSS for phase correction of aperture antennas [10, 11] is another important aspect for modern antenna engineering. Very recently FSSs have been designed also using artificial intelligence. For example, design of 3-D FSS using multiobjective lazy ant colony optimization algorithm [12], and multi-objective particle swarm optimization for the realization of a low profile bandpass FSS [13] have been studied. In recent era, with the fast development of wireless communication technology, the use of FSSs in telecommunication systems, wireless security systems, and for interference mitigation between adjacent wireless networks have been investigated. For these purposes, FSSs with multiple stopband and multiple passband characteristics are very useful.

Dual stopband characteristics can be achieved by using anchor-shaped loop FSS structure [14], four small square slots loaded with multiple stub resonators [15] with higher design complexity, circular loop type FSS [16], square ring and four stubs loaded dual substrate FSS [17] for GSM and LTE, and double

Received 14 April 2019, Accepted 26 June 2019, Scheduled 15 July 2019

* Corresponding author: Kaushik Mandal (kaushikrpe@gmail.com).

[1] Department of Electrical Engineering, Global Institute of Science & Technology, Haldia 721657, India. [2] Institute of Radio Physics and Electronics, University of Calcutta, Kolkata 700009, India. [3] St. Thomas' College of Engineering & Technology, Kolkata 700023, India. [4] DETS, University of Kalyani, West Bengal 741235, India

layer FSS [18] on glass substrate to protect WLAN bands 2.4–2.5 GHz and 4.98-5.825 GHz. Triple band-stop characteristics has been achieved using simple conducting elements on both sides [19], and here the design is simple and easily optimizable, but the angular stability is only up to 30°. A complex design based on a rectangular shaped synthetic resonator [20] is also proposed for triple stopband characteristics; however, its application is limited due to non-availability of the synthetic resonator.

In this present era, use of mobile phones and wireless gadgets is unavoidable. There has been growing public concern on possible adverse health effects due to electro-magnetic field (EMF) radiation from mobile towers and mobile handsets. There have been several studies [21, 22] suggesting either the presence or absence of risk to human beings from EMF radiation. The main areas of concern are the radiation emitted by base transceiver stations (BTS) and mobile handsets. Concerns have also been raised that continuous exposure to EMF radiation emanating from telecom towers causes harmful thermal and non-thermal health effects. So, it is essential to protect the users from the harmful radiations of these devices. Towards this important issue, a few efforts have been observed from the researchers working on FSS. Recently, an electromagnetic band gap array [23] has been used as phone case for suppression of mobile phone radiation exposure, but EBG is much more costly than FR4. Single band-stop characteristic can be achieved using a modified swastika unit cell [24] with more miniaturization and angular stability, but it is only for a single band. There are some valid issues such as size of the unit cell, number of dielectric layers, angular stability, and accurately covering the commercially useful frequency bands need to be considered during the design of FSSs.

Looking into the above issues we propose a very simple design which solves some of the above-mentioned issues. This paper shows that a single side single layer FSS with a pair of concentric square ring patches as a unit cell is able to exhibit multi band-stop characteristics covering the widely used frequency bands for mobile communications. Size of the unit cell is $0.140\lambda \times 0.140\lambda$, where λ is wavelength corresponding to the lowest operating frequency. The outer square ring provides 0.7–1.07 GHz stopband which covers GSM-900 and CDMA, and the inner square ring exhibits 1.68–2.79 GHz stopband which covers GSM-1800, LTE-2200 MHz, Wi-Fi, and Bluetooth bands. This proposed design also shows stable performance over a wide range of incidence angles. Hence, this novel dual band-stop FSS can be used to protect users from harmful radiations by GSM-900, CDMA, GSM-1800, LTE-2200 MHz, and 2.4 GHz signals. There are several research works on multiple stopband FSS design, but none of them have proposed such an easy and compact design along with design formula for these commercial bands. All the simulations are carried out using FEM-based Ansys HFSS EM simulator.

2. CIRCULAR RING TYPE FSS

The main goal of this work is to design an FSS based mobile radiation reflector to protect mobile phone user from harmful mobile radiations. This FSS based mobile radiation reflector must be kept in between the human body and mobile handset with a specified gap for the best protection. Such a system can be easily used along with the mobile case to carry it in the pocket. Back radiation from the mobile will be minimized whereas signal coverage and quality of the service between the mobile and base station will be least affected.

Both simulation and experimental investigations have been carried out extensively in a two-fold manner. Initially, a circular ring type FSS, as illustrated in Fig. 1, is studied. Next, a pair of square ring patches is used to replace the circular ring patches. The proposed structure is designed on a single side copper clad FR4 substrate of dimension $(70 \times 70 \times 1.6)\,\text{mm}^3$, $\varepsilon_r = 4.4$, and loss tangent of 0.02. Two metallic ring shaped patches are used, with outer ring radius $(R1) = 32$ mm, width $(W1) = 2$ mm, inner ring radius $(R2) = 20$ mm, and inner ring width $(W2) = 8$ mm.

Circular ring-shaped patch type FSS can be used as a band-stop filter for a particular resonance frequency with certain bandwidth. The resonating wavelength is nearly equal to the circumference of the circular ring [1]. So, different resonance frequencies can be achieved easily by changing the inner radius of the circular ring-shaped patch keeping the patch width fixed. Circular ring with higher radius provides lower resonating frequency, and lower radius patch resonates at higher frequency, as illustrated in Fig. 2. So, using this concept one can design an FSS to stop a particular frequency band as per the requirements.

Now using two or more concentric rings on a single substrate, multiple stopbands can be achieved,

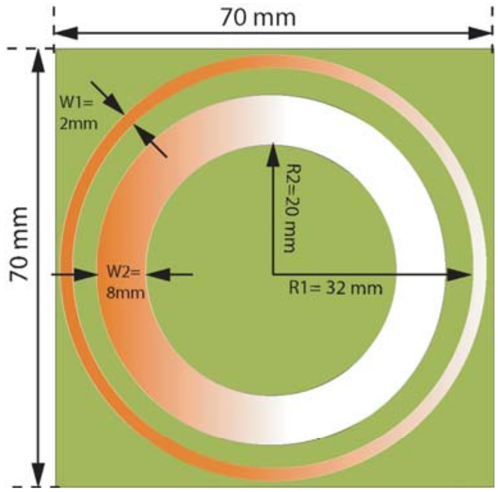

Figure 1. Geometry of patch type circular ring FSS.

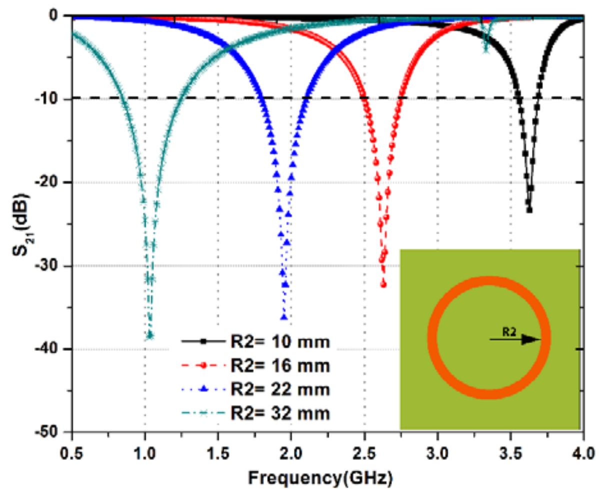

Figure 2. S_{21} curves for different radii ($R2$) of the single resonator circular ring, keeping the ring width (2 mm) fixed.

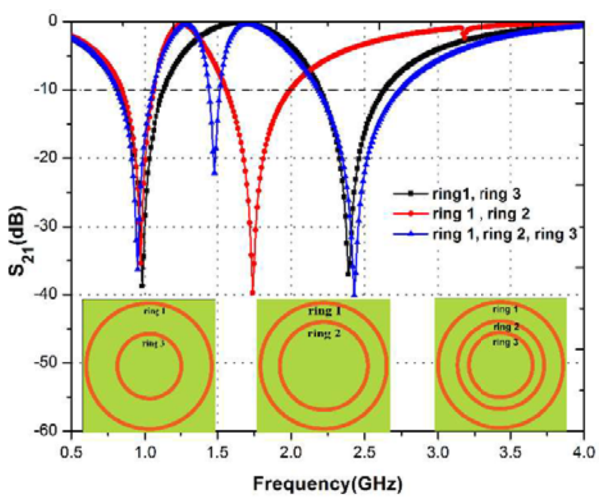

Figure 3. Effect on transmission coefficient for different configurations.

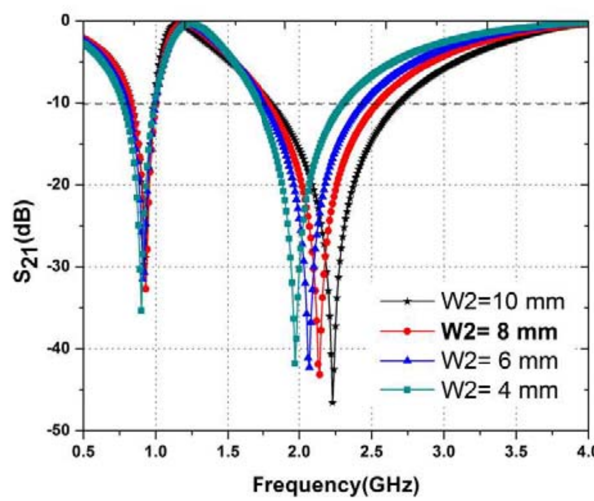

Figure 4. S_{21} curves for the variation of inner ring width ($W2$), keeping outer ring width ($W1 = 2$ mm) fixed.

as shown in Fig. 3. Two rings {(ring 1+ ring 3) and (ring 1 + ring 2)} with higher radius difference provides two separate bands, whereas for triple band operation if we use three rings (ring 1 + ring 2 + ring 3), the middle band is affected due to mutual coupling among the closely spaced rings (ring 2 and ring 3). So, the best way to minimize or to avoid the interference is to cover more closely spaced bands using a single resonator with larger width. As GSM-1800, LTE, Wi-Fi, and Bluetooth are very close frequency bands, a single resonator with larger width is conceived to cover all these bands in a single operating band.

The inner ring width ($W2$) variation is shown in Fig. 4. This parametric study helps us to select the optimum width of the inner ring as 8 mm in order to cover GSM-1800, LTE, Bluetooth, and Wi-Fi bands in a single operating band (1.75–2.54 GHz), whereas the outer ring of thickness 2 mm covers CDMA and GSM-900 bands.

3. SQUARE RING TYPE FSS

To find the performance comparison between the circular and square ring patch type FSSs, a same size square ring and a circular ring patch type FSS of dimension 70 mm × 70 mm are compared, and it is noticed that square ring FSS provides stopband around lower resonant frequency rather than circular ring FSS [23] as illustrated in Fig. 5. Therefore, square ring type FSS is more effective in the application area where size of the FSS is restricted to cover the lower range frequency bands.

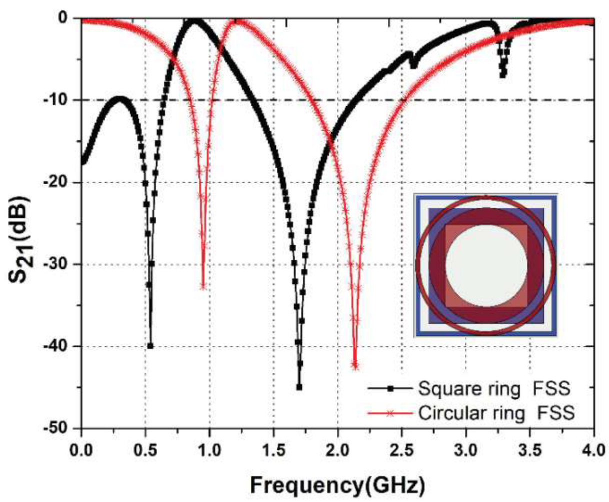

Figure 5. S_{21} curves for comparison of square and circular ring patch type FSS.

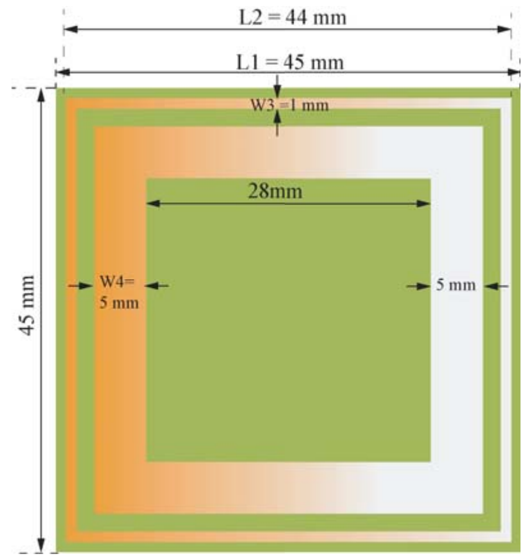

Figure 6. Geometry of square ring type FSS.

Now, considering this concept, a square ring type FSS of overall dimension 45 mm × 45 mm × 1.6 mm is designed using same substrate to cover the same frequency bands. Widths of the inner ring and outer ring are optimized to 5 mm and 1 mm, respectively, maintaining a gap of 2 mm between them. The top view of this proposed square ring patch type FSS is shown in Fig. 6.

The variation of resonance frequency with changing the inner dimension of the square ring is shown in Fig. 7, keeping other parameters fixed. It shows that higher dimension provides lower resonance frequency, and lower dimension exhibits higher resonance frequency. So, according to the requirement FSSs can be designed to stop different frequency bands as discussed in Section 2.

Square loop resonance occurs when the length of each half loop is a multiple of half-wavelength. In other words, each half-loop acts as a dipole element. The length of the whole loop needs to be a multiple of one full wavelength [25]. To calculate the resonance frequency of the stopband, a combination of the 1st and 2nd order empirical-formulas (1)–(4) is derived by applying linear regression analysis techniques [26] on the simulated data for a fixed width single circular ring (width = 2 mm) and a single square ring (width = 1 mm) patch type FSSs.

$$f_0(circular) = 4.644 - 0.0588D \tag{1}$$

$$f_0(circular) = 5.6207 - 0.115D + 0.0007D^2 \tag{2}$$

$$f_0(square) = 6.202 - 0.132D \tag{3}$$

$$f_0(square) = 7.511 - 0.2528D + 0.00233D^2, \tag{4}$$

where "D" is the internal distance of square ring and/or inner diameter of the circular ring.

These equations show the dependency of stopband resonance frequency on the inner diameter (circular ring)/internal distance (square ring) of the FSSs. The designed formula is verified with the simulated results as shown in Fig. 8. A strong similarity is observed for the second order Equations (2) and (4) with the simulated result for both the configurations of the FSSs.

Now to achieve multiple stopband characteristics, two or more rings of close resonance frequency can be used. The effect of number of ring variation and gap variation between the concentric square rings is illustrated in Fig. 9. If two rings of closely spaced resonance frequencies are used, then due to mutual coupling the stopband center frequency and operating band have been shifted slightly.

If three square rings are placed closely, then the middle band is affected badly, as illustrated in Fig. 9. So, instead of using individual resonator for an individual band we use only two square rings with different widths to minimize the coupling among the resonators. The inner ring width plays an important role to cover a wide stopband as shown in Fig. 10. This parametric study helps us to set the width of the inner ring as 5 mm.

Figure 11 shows comparison of the simulated and measured transmission coefficients for the proposed square ring patch type FSS. The surface current distributions in the inset of Fig. 12 ensure that the outer ring is responsible for the CDMA and GSM-900 bands, whereas the inner ring is responsible

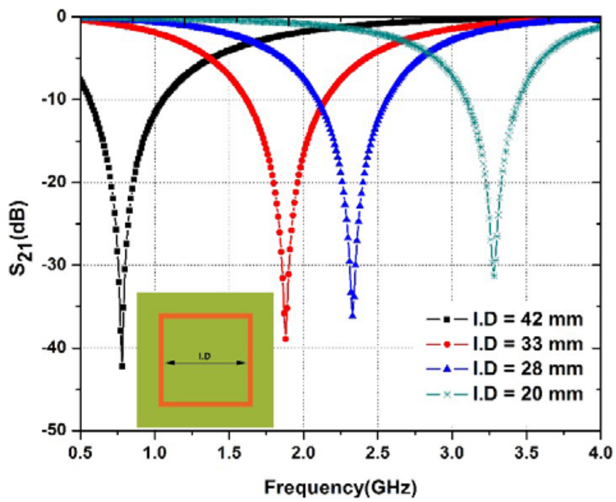

Figure 7. S_{21} curves for square ring for different internal distance (I.D) of the ring keeping the ring width (1 mm) fixed.

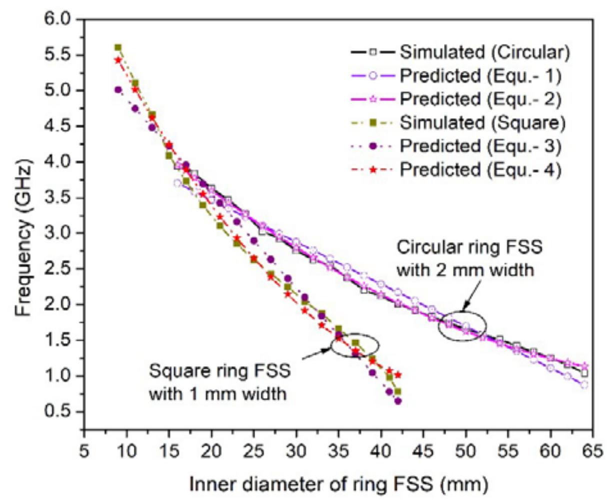

Figure 8. Stopband resonance frequency variation with inner diameter variation of patch type ring FSSs.

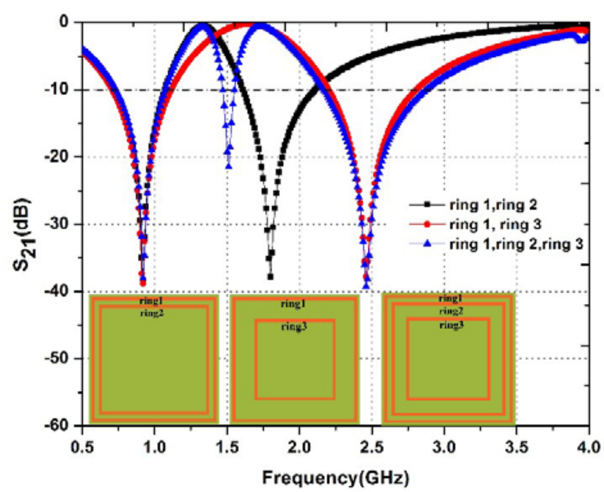

Figure 9. S_{21} curves for different arrangement of square ring FSS, keeping rings width fixed.

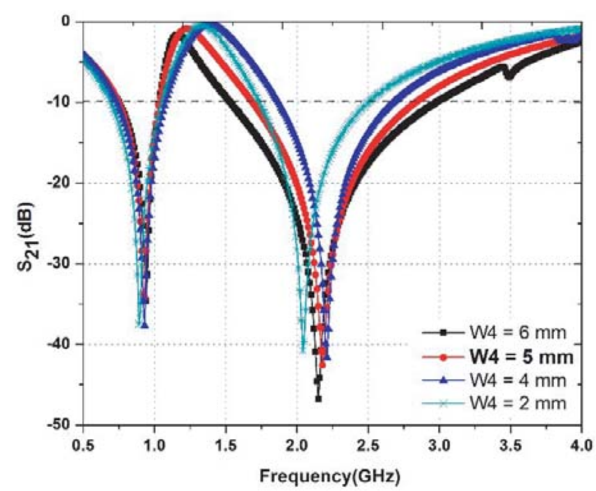

Figure 10. Effect on the S_{21} for variation of inner ring width ($W4$) of square ring resonator, keeping outer ring width ($W3 = 1$ mm) fixed.

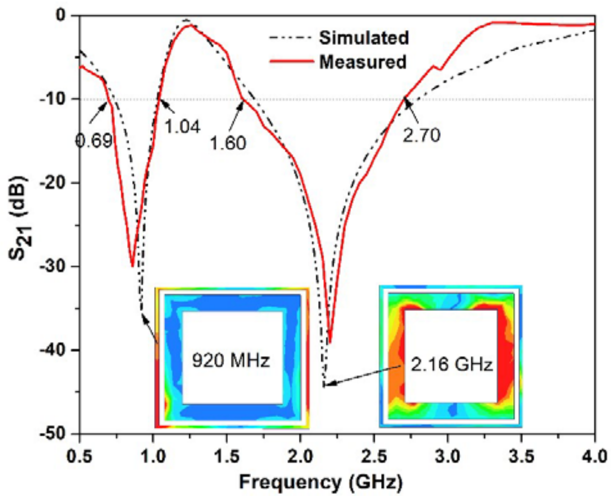

Figure 11. Comparison of the simulated and measured transmission coefficient (S_{21}) for the proposed square ring patch type FSS.

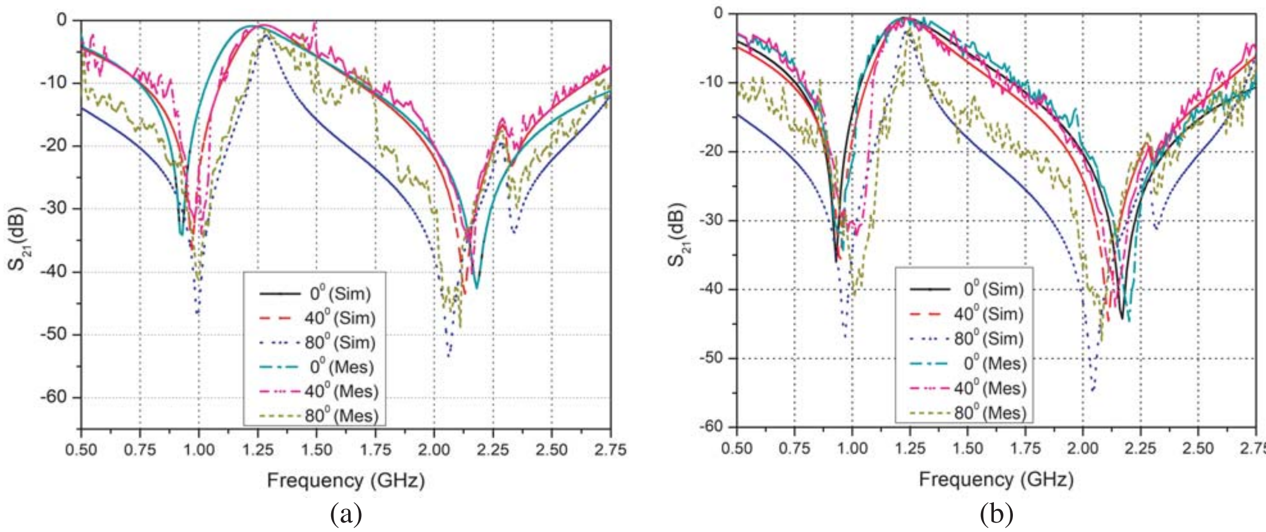

Figure 12. Comparison of simulated and measured S_{21} curves for different incidence angle under (a) TE mode and, (b) TM mode.

for the GSM-1800, LTE, Bluetooth, and Wi-Fi bands.

FSS is installed in a particular place for a specific application, and it can be illuminated by different signals with different incidence angles. So, a good FSS should show stable response for different incidence angles. The simulated and measured S_{21} curves for different incidence angles under TE and TM polarizations are shown in Fig. 12. The results show almost stable responses for 0° to 80° with a step of 20°. A slight change of center frequency has been observed for the incidence angle 60° onwards, but as the desired stopband is not affected, this little change can be neglected. Due to the fabrication tolerances and measurement environment, the measured S_{21} curves slightly deviate from the simulated one. The obtained results approve the expected higher angular stability characteristic of the proposed design. Hence, the claim for angular stability 0° to 80° has been made.

The previous section describes the frequency response for the unit cell only, but as the practical FSS consists of array of finite number of unit cells, the proposed design is analyzed with 3×3 and 6×6 configurations, and it shows nearly symmetrical response, as illustrated in Fig. 13. For wave-port analysis, E-planes are placed opposite to each other, and H-planes are placed opposite to each other.

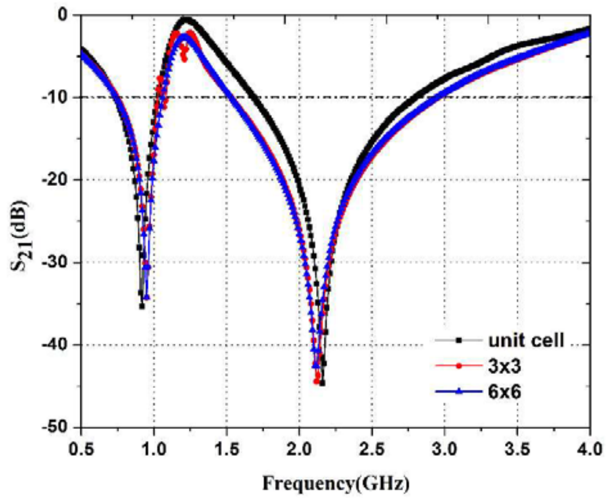

Figure 13. Simulated S_{21} curve for different array size.

The periodicity of the printed pattern is kept much smaller than the wavelength of the corresponding operating frequency. To avoid grating lobes, the periodicity is kept less than 0.5λ.

4. MEASURED RESULTS AND DISCUSSIONS

Considering the optimized dimensions as per the earlier section, a prototype of the square ring type 6×6 FSS is fabricated and measured in the antenna and microwave laboratory to verify the FSS performance in filtering application. The measured transmission coefficient shows good agreement with the simulated one, as depicted in Fig. 11, and it provides band-stop characteristics over the 0.69–1.04 GHz and 1.60–2.70 GHz frequency bands.

The band-stop characteristics of the fabricated FSS have been tested using HTC EMF-523 Radio Active Electro Magnetic Field Tester Meter. The radiations from Mi Wi-Fi router and Mi 4i mobile are considered to test the effectiveness of the designed FSS around 2.4 GHz and GSM bands (GSM-900 and GSM-1800), respectively. The radiation power densities from a Mi Wi-Fi router have been measured using the EMF tester in absence and presence of FSS in between the tester and router. The EMF tester is kept just behind the FSS, and then the FSS is kept at various distances from the router. The measurement setup is shown in Fig. 14, and the results are summarized in Table 1.

(a) (b)

Figure 14. Measurement of power density of Mi Wi-Fi router, (a) without FSS, and (b) with FSS.

Table 1. Radiation power density measurement of Mi Wi-Fi router.

Distance between EMF tester and Wi-Fi router (mm)	Measured radiation power density (mW/m^2)	
	Without FSS	With FSS
20	842.7	66.43
100	579.5	48.5
250	410.3	7.68

A similar test has also been carried out with Mi 4i mobile. The corresponding measurement setup is shown in Fig. 15, and the results are summarized in Table 2. It has been observed that the radiation power densities fall drastically in the presence of the FSS in both the cases, and it ensures the effectiveness of the proposed FSS as a good candidate to reduce mobile phone radiation exposure.

(a) (b)

Figure 15. Measurement of power density of Mi 4i Mobile (a) without FSS, and (b) with FSS.

Table 2. Radiation power density measurement of Mi 4i mobile.

Distance between EMF tester and Mobile (mm)	Measured radiation power density (mW/m^2)	
	Without FSS	With FSS
Attached to the back of mobile phone	1155.3	105.94
100	800.3	60.5
250	535.5	15.7

To show advantages of the proposed FSS over similar previously designed FSSs, a comparative study is carried out and summarized in Table 3. The comparison is done based on the unit cell size, number of useful bands covered, operating frequency bands, and incidence angle stability. Critical analysis of Table 3 shows that the proposed FSS is able to cover maximum number of useful bands with maximum level of angular stability. Though the unit cell size of [24] is less, it covers only a single useful band and exhibits lower angular stability than the proposed design.

To date, a few efforts have been observed to design a simple FSS based mobile back cover. A very simple single-layer FSS with a pair of concentric square ring patches is able to exhibit multi band-stop characteristics covering the mobile frequency bands. Using two or more concentric rings on a single substrate, multiple stopbands can be achieved easily, but due to mutual coupling among the closely

Table 3. Performance comparison of the proposed design with some of the existing designs.

FSS design	Unit cell size	No. of useful bands covered	Operating frequency bands	Angular stability	
				Incidence angle	Max. deviation (GHz)
[16]	0.234 λ (single side)	2	2.4 GHz and 5.8 GHz band	0° to 60°	Approx. 0.25
[19]	0.166λ (double side)	3	WiMAX, WLAN, and X band	0° to 50°	NA
[20]	0.157 λ (single side)	3	GSM-900, GSM-1800, 2142 MHz	NA	NA
[24]	0.117λ (single side)	1	5-GHz WLAN	0° to 60°	0
Proposed design	**0.140 λ (single side)**	**5**	**CDMA, GSM-900, GSM1800, LTE-2200, 2.4 GHz**	0° **to** 80°	**0.12**

spaced rings, the operating bands are affected. So, to avoid the interference the solution is to cover a number of closely spaced bands using a single resonator with a larger width. This concept greatly helps to maintain the required compactness of the proposed design. Further, generalized design formulas for the band stop FSS design have been proposed using linear polynomial regression techniques.

5. CONCLUSION

A very simple multiple stopband FSS for the GSM-900, CDMA, GSM-1800, LTE-2200 MHz, and Bluetooth is studied thoroughly. Initially, the possibilities of the circular ring FSS has been explored, but the square ring type FSS exhibits 58.67% compactness in comparison to the circular ring FSS, so finally, the square ring-type FSS has been designed and analyzed. Instead of using multiple resonators for the individual bands, a single resonator with larger width is used to cover closely spaced frequency bands, and another square ring with larger length and lower width is used to cover lower frequency bands for mobile application. Considering the transmission characteristic of this proposed FSS, it can be suitable for the suppression of mobile phone radiation exposure and will be able to protect the mobile phone users from its harmful radiations.

REFERENCES

1. Munk, B. A., *Frequency Selective Surfaces: Theory and Design*, Wiley, New York, 2000.
2. Barton, J. H., C. R. Garcia, E. A. Berry, R. Salas, and R. C. Rumpf, "3-D printed all-dielectric frequency selective surface with large bandwidth and field of view," *IEEE Trans. Antennas Propag.*, Vol. 63, 1032–1039, 2015.
3. Lalbakhsh, A., M. U. Afzal, K. P. Esselle, and S. L. Smith, "Wideband near-field correction of a fabry-perot resonator antenna," *IEEE Trans. Antennas Propag.*, Vol. 67, 1975–1980, 2019.
4. Afzal, M. U., A. Lalbakhsh, and K. P. Esselle, "Electromagnetic-wave beam-scanning antenna using near-field rotatable graded-dielectric plates," *Journal of Applied Physics*, Vol. 124, 234901–234911, 2018.
5. Mackay, A., B. Sanz-Izquierdo, and E. A. Parker, "Evolution of frequency selective surfaces," *Forum for Electromagnetic Research Methods and Application Technologies (FERMAT)*, Vol. 2, 1–7, 2014.
6. Nair, R. U. and R. M. Jha, "Electromagnetic design and performance analysis of airborne radomes: Trends and perspectives antenna applications corner," *Antennas Propag. Mag.*, Vol. 56, No. 4, 276–298, 2014.
7. Luukkonen, O., F. Costa, C. R. Simovski, A. Monorchio, and S. A. Tretyakov, "A thin electromagnetic absorber for wide incidence angles and both polarizations," *IEEE Trans. Antennas Propag.*, Vol. 57, No. 10, 3119–3125, Oct. 2009.

8. Zahirjoozdani, M., M. Khalajamirhosseini, and A. Abdolali, "Wideband radar cross-section reduction of patch array antenna with miniaturized hexagonal loop frequency selective surface," *Electron. Lett.*, Vol. 52, No. 9, 767–768, 2016.
9. Hiranandani, M. A., A. B. Yakovlev, and A. A. Kishk, "Artificial magnetic conductors realised by frequency-selective surfaces on a grounded dielectric slab for antenna applications," *IEE Proceedings — Microwaves, Antennas and Propagation*, Vol. 153, 487–493, 2006.
10. Lalbakhsh, A., M. U. Afzal, K. P. Esselle, S. L. Smith, and B. A. Zeb, "Single-dielectric wideband partially reflecting surface with variable reflection components for realization of a compact high-gain resonant cavity antenna," *IEEE Trans. Antennas Propag.*, Vol. 67, 1916–1921, 2019.
11. Lalbakhsh, A., M. U. Afzal, and K. P. Esselle, "Multiobjective particle swarm optimization to design a time-delay equalizer metasurface for an electromagnetic band-gap resonator antenna," *IEEE Antennas and Wireless Propag. Lett.*, Vol. 16, 912–915, 2017.
12. Zhu, D. Z., P. L. Werner, and D. H. Werner, "Design and optimization of 3-D frequency-selective surfaces based on a multiobjective lazy ant colony optimization algorithm," *IEEE Trans. Antennas Propag.*, Vol. 65, 7137–7149, 2017.
13. Lalbakhsh, A., M. U. Afzal, K. P. Esselle, and B. A. Zeb, "Multi-objective particle swarm optimization for the realization of a low profile bandpass frequency selective surface," *International Symposium on Antennas and Propagation (ISAP)*, Hobart, TAS, Australia, Nov. 9–12, 2015.
14. Yan, M.. S. Qu, J. Wang, and H. Zhou, "A miniaturized dual-band FSS with stable resonant frequencies of 2.4 GHz/5 GHz for WLAN applications," *IEEE Antennas and Wireless Propag. Lett.*, Vol. 13, 895–898, 2014.
15. Rahmati, B. and H. R. Hassani, "Multiband metallic frequency selective surface with wide range of band ratio," *IEEE Trans. Antennas Propag.*, Vol. 63, 3747–3753, 2015.
16. Döken, B. and M. Kartal, "Easily optimizable dual-band frequency selective surface design," *IEEE Antennas and Wireless Propag. Lett.*, Vol. 16, 2979–2982, 2017.
17. Dai, X.-W. and T. Zhou, "Dual-band reflect array with crossed-dipole elements for GSM and LTE applications," *AEU — International Journal of Electronics and Communications*, Vol. 70, 605–610, 2016.
18. Bagci, F., C. Mulazimoglu, S. Can, E. Karakaya, A. Egemen Yilmaz, and B. Akaoglu, "A glass based dual band frequency selective surface for protecting systems against WLAN signals," *AEU — International Journal of Electronics and Communications*, Vol. 82, 426–434, 2017.
19. Bashiri, M., C. Ghobadi, J. Nourinia, and M. Majidzadeh, "WiMAX, WLAN, and X-band filtering mechanism: Simple-structured triple-band frequency selective surface," *IEEE Antennas and Wireless Propag. Lett.*, Vol. 16, 3245–3248, 2017.
20. Kartal, M., J. J. Golezani, and B. Doken, "A triple band frequency selective surface design for GSM systems by utilizing a novel synthetic resonator," *IEEE Trans. Antennas Propag.*, Vol. 65, 2724–2727, 2017.
21. Yang, L. and L. Guizhen, "The research on biological effects of mobile phone radiation to human body," *Proceedings of 2008 Asia-Pacific Microwave Conference*, 1–4, Macau, China, 2008.
22. Yaning, L., "Review on the investigation of the mechanism of the biological effects of the electromagnetic radiation," *Basic Medical Sciences and Clinics*, Vol. 20, No. 1, 21–23, 2000.
23. Da, R. and H. Yoo, "Application of a compact electromagnetic bandgap array in a phone case for suppression of mobile phone radiation exposure," *IEEE Transactions on Microwave Theory and Techniques*, Vol. 66, 2363–2372, 2018.
24. Natarajan, R., M. Kanagasabai, S. Baisakhiya, R. Sivasamy, S. Palaniswamy, and J. K. Pakkathillam, "A compact frequency selective surface with stable response for WLAN applications," *IEEE Antennas and Wireless Propag. Lett.*, Vol. 12, 718–720, 2013.
25. Wu, T. K., *Frequency Selective Surface and Grid Array: Wiley series in Microwave and Optical Engineering*, New York, Jul. 1995.
26. Chatterjee, S. and A. S. Hadi, *Regression Analysis by Example*, John Wiley & Sons, New Jersey, 2006.